Mechanisms of Benzene-Induced Hematotoxicity and Leukemogenicity: cDNA Microarray Analyses Using Mouse Bone Marrow Tissue

Byung-IL Yoon,[1] Guang-Xun Li,[1] Kunio Kitada,[2] Yasushi Kawasaki,[1] Katsuhide Igarashi,[1] Yukio Kodama,[1] Tomoaki Inoue,[2] Kazuko Kobayashi,[2] Jun Kanno,[1] Dae-Yong Kim,[3] Tohru Inoue,[4] and Yoko Hirabayashi[1]

[1]Division of Cellular and Molecular Toxicology, National Institute of Health Sciences, Tokyo, Japan; [2]Kamakura Research Labs, Chugai Pharmaceutical, Co., Ltd., Kamakura, Japan; [3]Department of Veterinary Pathology, College of Veterinary Medicine and Agricultural Biotechnology, Seoul National University, Seoul, Republic of Korea; [4]Biological Safety and Research Center, National Institute of Health Sciences, Tokyo, Japan

Although the mechanisms underlying benzene-induced toxicity and leukemogenicity are not yet fully understood, they are likely to be complicated by various pathways, including those of metabolism, growth factor regulation, oxidative stress, DNA damage, cell cycle regulation, and programmed cell death. With this as a background, we performed cDNA microarray analyses on mouse bone marrow tissue during and after a 2-week benzene exposure by inhalation. Our goal was to clarify the mechanisms underlying the hematotoxicity and leukemogenicity induced by benzene at the level of altered multigene expression. Because a few researchers have postulated that the cell cycle regulation mediated by p53 is a critical event for benzene-induced hematotoxicity, the present study was carried out using p53-knockout (KO) mice and C57BL/6 mice. On the basis of the results of large-scale gene expression studies, we conclude the following: *a*) Benzene induces DNA damage in cells at any phase of the cell cycle through myeloperoxidase and in the redox cycle, resulting in *p53* expression through *Raf-1* and cyclin D-interacting myb-like protein 1. *b*) For G1/S cell cycle arrest, the p53-mediated pathway through p21 is involved, as well as the pRb gene–mediated pathway. *c*) Alteration of *cyclin G1* and *Wee-1 kinase* genes may be related to the G2/M arrest induced by benzene exposure. *d*) DNA repair genes such as *Rad50* and *Rad51* are markedly downregulated in p53-KO mice. *e*) p53-mediated caspase 11 activation, aside from p53-mediated *Bax* gene induction, may be an important pathway for cellular apoptosis after benzene exposure. Our results strongly suggest that the dysfunction of the *p53* gene, possibly caused by strong and repeated genetic and epigenetic effects of benzene on candidate leukemia cells, may induce fatal problems such as those of cell cycle checkpoint, apoptosis, and the DNA repair system, finally resulting in hemopoietic malignancies. Our cDNA microarray data provide valuable information for future investigations of the mechanisms underlying the toxicity and leukemogenicity of benzene. *Key words:* apoptosis, benzene, cDNA microarray, cell cycle, DNA damage, DNA repair, hematotoxicity, leukemia, oxidative stress, p53-knockout mice. *Environ Health Perspect* 111:1411–1420 (2003). doi:10.1289/txg.6164 available via *http://dx.doi.org/* [Online 5 August 2003]

Benzene is well documented as an environmental pollutant that can induce hematotoxicity and hemopoietic neoplasia in humans and mice (Aksoy et al. 1974, 1976; Cronkite et al. 1984, 1989; Snyder et al. 1980; Vigliani and Forni 1976). To date, studies on benzene have focused on its metabolic pathways to determine the metabolites responsible for its hematotoxicity and leukemogenicity (Henderson 1996; Schlosser et al. 1989; Schrenk et al. 1996; Snyder and Hedli 1996). Benzene and its major metabolites are not mutagenic in the Ames *Salmonella* test (Dean 1985), but they do induce chromosomal aberration both *in vitro* and *in vivo* (Dean 1985; Wolman 1977; Yager et al. 1990). This is comparable to classic carcinogens that are generally being activated to a single carcinogenic metabolite having a mutagenic property. Benzene can be characterized further in terms of its multisite carcinogenicity (Huff et al. 1989; Maltoni et al. 1989). Mice exposed to benzene develop different types of tumor in various glandular tissues and organs, including the hemopoietic system, Zymbal gland, Harderian gland, preputial gland, mammary gland, ovary, and lung. Results of the study of Low et al. (1995) strongly suggest that the carcinogenicity of benzene on target organs depends on the ability of enzymes in the organs to metabolize benzene.

As postulated by several investigators, the metabolism of benzene to reactive metabolites by hepatic enzymes, mainly cytochrome P450-2E1 (CYP2E1), is a prerequisite to the cyto- and genotoxicities associated with benzene exposure (Gut et al. 1996; Snyder and Hedli 1996; Valentine et al. 1996). Primary benzene metabolites include phenol, hydroquinone, catechol, and *trans-trans* muconic acid (Ross 2000). The synergistic interactions between these phenolic metabolites exacerbate benzene toxicity (Chen and Eastmond 1995; Eastmond et al. 1987; Subrahmanyam et al. 1990). This mechanism of multimetabolite genotoxicity is another unique aspect of benzene that distinguishes it from other chemicals in terms of the mechanism of its toxicity and carcinogenicity. Benzene metabolites subsequently undergo secondary activation by myeloperoxidase (MPO) that is present at high levels in the bone marrow tissue. This results in the production of genotoxic quinones and reactive oxygen species, thereby inducing not only hemopoietic cellular damage (Farris et al. 1997; Kolachana et al. 1993; Lee and Garner 1991; Smith et al. 1989) but also the dysfunction of bone marrow stromal cells (Niculescu et al. 1995).

Exposure duration and dose are also important factors in determining benzene-induced hematotoxicity and leukemogenicity (Cronkite et al. 1989; Snyder and Kalf 1994), which may be related to the limited capacity of enzymes for benzene metabolism and to the dynamic responses of hemopoietic microenvironmental conditions against the adverse effects of benzene.

Despite intensive studies over several decades, the mechanisms underlying benzene-induced hematotoxicity and leukemogenicity are still not fully understood. Nevertheless, previous studies strongly suggest that the toxic effects of benzene on bone marrow tissue can be realized through pathways such as those of metabolism (Snyder and Hedli 1996), growth factor regulation (Niculescu et al. 1995),

Address correspondence to Y. Hirabayashi, Division of Cellular and Molecular Toxicology, Biological Safety and Research Center, National Institute of Health Sciences, 1-18-1 Kamiyoga, Setagayaku, Tokyo 158-8501 Japan. Telephone: 81 3 3700 9639. Fax: 81 3 3700 9647. E-mail: yokohira@nihs.go.jp

We thank E. Tachihara, Y. Usami, and Y. Shinzawa for their excellent technical assistance and N. Katsu and Y. Nagano for their help in manuscript preparation. We also thank the late E. Cronkite for constructive discussion and comments on the manuscript.

This work was supported by the Japan Health Sciences Foundation (research on health sciences focusing on drug innovation, KH31034).

The authors declare they have no conflict of interest.

Received 17 December 2002; accepted 10 July 2003.

production of oxidative stress (Laskin et al. 1996; Subrahmanyam et al. 1991), DNA damage and repair (Lee and Garner 1991), cell cycle regulation (Yoon et al. 2001b), and apoptosis (Moran et al. 1996; Ross et al. 1996). These studies indicate that investigation of the roles of a few specific genes may not be sufficient to explain the complete molecular mechanism of benzene-induced hematotoxicity and leukemogenicity.

Bone marrow tissue, a major target organ of benzene, is an active hemopoietic system in which various counterbalanced genes are organized through their network interactions that maintain cellular–environmental homeostasis as well as protect cells from endogenous and exogenous hematotoxic effects such as benzene-induced effects. The dysregulation of such a multidimensional counterbalance, possibly induced by the genetic and epigenetic effects of benzene, may result in the altered expression of a number of genes associated with the mechanisms of benzene-induced hematotoxicity and leukemogenicity.

In this study we investigated the changes in DNA expression during and after benzene exposure (300 ppm) to probe further the molecular mechanisms underlying benzene toxicity. Because previous studies (Boley et al. 2002; Yoon et al. 2001b) demonstrated that the *p53* tumor suppressor gene is important in cell cycle regulation associated with the mechanisms of benzene-induced toxicity, these analyses were carried out by cDNA microarray analyses in C57BL/6, wild-type (WT), and p53-knockout (KO) mice.

Materials and Methods

Animals

Specific pathogen–free, 7-week-old, male C57BL/6 mice were purchased from Japan SLC (Hamamatsu, Japan) and quarantined for 1 week in 1.3-m^3 inhalation chambers (Shibata Scientific Technology Ltd., Tokyo, Japan) in ambient air. To obtain WT and p53-KO mice for use in this study, male and female heterozygous p53-KO C57BL/6 mice, originally bioengineered by Tsukada et al. (1993), were mated; the pups produced were then identified by polymerase chain reaction analysis of the DNA samples extracted from the tail of each mouse. The mice were grouped randomly into untreated control and benzene-exposed groups and maintained in stainless-steel wire cages inside inhalation chambers under a 12-hr light–dark cycle during the study. A basic pellet diet (CRF-1; Funabashi Farm, Funabashi, Japan) was provided *ad libitum* except during the daily 6-hr benzene inhalation period. Water was delivered by an automated tubing nozzle and provided *ad libitum* throughout the study.

Benzene Exposure

Benzene vapor was generated and its concentration was monitored as described elsewhere (Yoon et al. 2001b). Temperature and humidity inside the chambers were maintained automatically at 24 ± 1°C and 55 ± 10%, respectively. Mice were exposed to 300 ppm benzene for 6 hr/day, 5 days/week for 2 weeks; the sham control groups were maintained in the inhalation chambers in ambient air over the same period. Experimental schedules for sham and benzene-treated mice are shown in Figure 1. Immediately after the first 5 days of exposure (D5), the second 5 days of exposure in the second week (D12), and 3 days after D12 for recovery (D+3), the mice were sacrificed. D12 is also designated as the 2-week exposure. To investigate changes in gene expression, three C57BL/6 mice from each of the sham control and benzene-exposed groups were decapitated after euthanasia at 1 week (D5) and 2 weeks (D12), respectively, during a 2-week benzene exposure period and 3 days after benzene removal (D+3), and poly(A)$^+$ RNA extracted from each group was applied to Incyte gene expression microarray (GEM) assay (Incyte Pharmaceuticals, Inc., Palo Alto, CA, USA) (see "Microarray Preparation"). Our previous study (Yoon et al. 2001b) showed that mice are able to recover from benzene-induced hematotoxicity 3 days after a 2-week benzene exposure. In studies using WT and p53-KO mice, two to four mice from each group and genotype were sacrificed immediately after the 2-week benzene exposure and applied to the Affymetrix system (Affymetrix, Inc., Santa Clara, CA, USA) (see "Microarray Preparation").

Bone Marrow Cell Collection for RNA Extraction

The mice from which bone marrow cells were collected for RNA extraction were carefully chosen on the basis of our evaluation of peripheral blood number and bone marrow cellularity using a blood cell counter (Sysmex M-2000; Sysmex Co., Tokyo, Japan) and our comparison of the values with those previously reported (Yoon et al. 2001b).

We harvested bone marrow cells from both femurs of individual mice of each group (Yoon et al. 2001b). Using a 27-gauge hypodermic needle, we flushed out bone marrow cells of the bone shafts with 2 mL Dulbecco's modified minimum essential medium without phenol red (Invitrogen Corp., Carlsbad, CA, USA). Single-cell suspensions were then prepared by repeatedly passing the harvested bone marrow cells through the needle. After the lysis of red blood cells, the bone marrow cells were immediately frozen in liquid nitrogen and stored at –80°C until RNA extraction.

Preparation of Total RNA and Poly(A)$^+$ RNA

Total RNA was extracted from the collected bone marrow cells using ISOGEN (Wako Chemical Co., Osaka, Japan) in accordance with the manufacturer's instructions. The total RNA yielded optical density (OD) ratios (OD 260/280) of 1.7–2.1; its purity was confirmed by gel

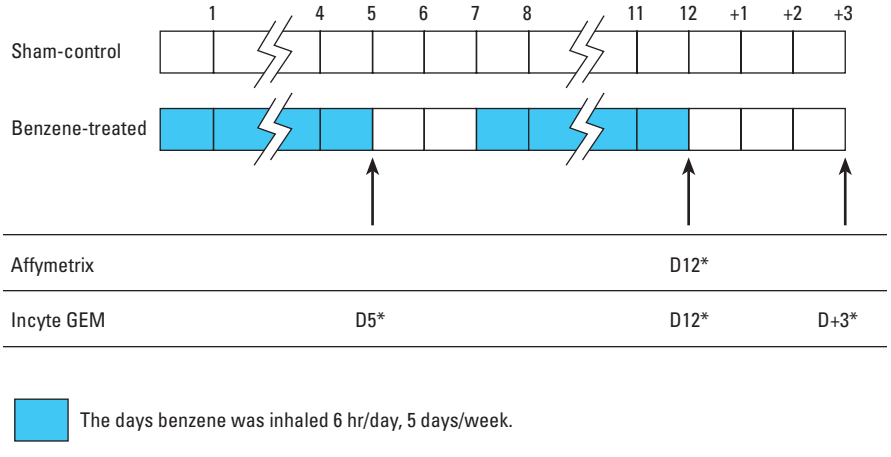

Figure 1. Benzene inhalation schedule diagram: exposure was for 6 hr/day from 10 A.M. to 4 P.M. On the days marked with an asterisk (*), both sham exposure mice were killed at 4 P.M., and exposed mice were killed immediately after exposure (Yoon et al. 2002). On D+3, both sham and recovery mice were killed at 4 P.M. D5 designates practically a 1-week exposure and D12, a 2-week exposure. D+3 is the group with a 3-day recovery period after D12.

chromatography, and its concentration was determined on the basis of its absorbance at 260 nm that was measured with a Beckman spectrophotometer (DU640; Beckman Coulter, Inc., Fullerton, CA, USA). Independent total RNA and poly(A)$^+$ RNA samples were separately extracted from three C57BL/6 mice and two to four WT and p53-KO mice; those samples from equivalent materials were analyzed using the Incyte GEM system and the Affymetrix system. We used the Affymetrix system to analyze further two separate RNA samples from benzene-exposed and sham-exposed WT mice at each time point, and two separate RNA samples from benzene-exposed and four separate samples from sham-exposed p53-KO mice. In addition, for further comparison, RNA samples from three mice in each of the four groups were pooled and processed with the Incyte GEM system. No duplicate or triplicate runs were performed using the Incyte GEM system. Poly(A)$^+$ RNA was prepared from the total RNA using Oligo (dT) Microbeads (Daiichi Co., Tokyo, Japan) in accordance with the manufacturer's instructions.

Microarray Preparation

All procedures such as experimental design, array design, sampling, hybridization, signal measurements, and normalization control were performed according to the MIAME (minimum information about a microarray experiment) guidelines (Brazma et al. 2001).

Affymetrix system. **Target preparation from total mRNA.** We synthesized the first-strand cDNA by incubating 40 μg total RNA with 400 U SuperScript II reverse transcriptase (Invitrogen), 100 pmol T7-$(dT)_{24}$ primer [5′-GGCCAGTGAATTGTAATACGACTCACTATAGGGAGGCGG-$(dT)_{24}$-3′], 1× first-strand cDNA synthesis buffer [50 mM Tris-HCl (pH 8.3), 75 mM KCl, 3 mM $MgCl_2$, and 10 mM dithiothreitol (DTT)], and 0.5 mM deoxynucleoside 5′-triphosphate [dNTP: mixture of 0.5 mM each deoxydenosine 5′-triphosphate (TP), deoxycytidine TP, deoxyguanosine TP, and deoxythymidine TP] at 42°C for 1 hr. We synthesized the second-strand cDNA by incubating the first-strand cDNA with 10 U *Escherichia coli* ligase (Invitrogen), 40 U DNA polymerase I (Invitrogen), 2 U RNase H (Invitrogen), 1× reaction buffer [18.8 mM Tris-HCl (pH 8.3), 90.6 mM KCl, 4.6 mM $MgCl_2$, 3.8 mM DTT, 0.15 mM nicotinamide adenine dinucleotide, and 10 mM $(NH_4)_2SO_4$], and 0.2 mM dNTP at 16°C for 2 hr. Ten units T4 DNA polymerase (Invitrogen) was added, and the reaction was allowed to continue for another 5 min at 16°C to generate the blunt-ended double-stranded (ds) cDNAs. After phenol/chloroform extraction and ethanol precipitation, the ds-cDNA was resuspended in 12 μL diethyl pyrocarbonate-treated distilled water. Biotin-labeled cRNAs were synthesized by *in vitro* transcription using a BioArray HighYield RNA transcript labeling kit (Enzo Diagnostics, Farmingdale, NY, USA). The ds-cDNA was then mixed with 1× HighYield reaction buffer, 1× mixture solution of four nucleoside TPs (NTPs: adenosine TP, cytidine TP, guanosine TP, and uridine TP) with biotin-labeled uridine TP and cytidine TP, 1× DTT, 1× RNase inhibitor mix, and 1× T7 RNA polymerase. The mixture was incubated at 37°C for 4 hr, with gentle mixing every 30 min. The labeled cRNA was then purified using an RNeasy minikit (Qiagen, Valencia, CA, USA) in accordance with manufacturer instructions. The purified cRNA was then fragmented in 1× fragmentation buffer (40 mM Tris–acetate, 100 mM potassium acetate, and 30 mM magnesium acetate) at 94°C for 35 min.

Hybridization and scanning. For hybridization, 15 μg of the fragmented cRNA probe was incubated with 50 pM control oligonucleotide B2, 1× eukaryotic hybridization control (1.5 pM *BioB*, 5 pM *BioC*, 25 pM *BioD*, and 100 pM *cre*), 0.1 mg/mL herring sperm DNA, 0.5 mg/mL acetylated bovine serum albumin, and 1× hybridization buffer in a 45°C rotisserie oven for 16 hr.

Probe array washing, staining, and antibody amplification. After hybridization, washing and staining were performed with a GeneChip fluidic station (Affymetrix) using appropriate antibody amplification washing and staining protocols.

Probe array scanning. The phycoerythrin-stained array was performed with a confocal scanner (Agilent Affymetrix GeneArray scanner), processed into digital image files, and analyzed using the Affymetrix analysis software Microarray Suite (MAS, version 4.0).

Data normalization. GeneSpring software (Silicon Genetics, Redwood City, CA, USA) was used to normalize the data. The 50th percentile of all measurements was used as a positive control for the sample; each measurement for each gene was divided by this synthetic positive control, assuming that this was at least 10. The bottom 10th percentile was used as a test for correcting background subtraction. This was never less than the negative values of the synthetic positive control. The measurement for each gene in each sample was divided by the corresponding mean of the sham controls, assuming that the cutoff value is more than 0.01.

Incyte GEM system. **Fluorescence labeling of probe for GEM system.** For comparison of the array data obtained using the Affymetrix system, the samples were simultaneously sent to the Incyte GEM system to analyze the time course of gene expression changes after benzene inhalation and its cessation. Poly(A)$^+$ RNA (200 ng) from each sample was sent to Incyte Co Ltd. (MouseUniGEM: GEM-5200; Fremont, CA, USA) via GEM custom screening services (Kurabo Co Ltd., Osaka, Japan). Briefly, the samples were incubated for 2 hr at 37°C with 200 U M-MLV reverse transcriptase (Life Technologies, Gaithersburg, MD, USA), 4 mM DTT, 1 U RNase inhibitor (Ambion, Austin, TX, USA), 0.5-mM dNTPs, and 2 μg 5′Cy3 or Cy5-labeled 9-mers (Operon Technologies Inc., Alameda, CA, USA) in 25-μL volume with an enzyme buffer supplied by the manufacturer, and then reverse-transcribed to cDNA. The reaction was terminated by heating at 85°C for 5 min. The paired reaction mixtures were combined and purified with a TE-30 column (Clonetech, Palo Alto, CA, USA), diluted to 90 μL with distilled water, and precipitated with 2 μL of 1 g/mL glycogen, 60 μL of 5 M ammonium acetate, and 300 μL ethanol. After centrifugation, the supernatant was decanted and the pellet was resuspended in 24 μL hybridization buffer, 5× sodium chlorine–sodium citrate buffer, 0.2% sodium dodecyl sulfate, and 1 mM DTT.

Hybridization. The probe solutions were thoroughly resuspended by incubating them at 65°C for 5 min, with mixing. The probe was applied to the array and covered with a 22-mm^2 glass cover slip and placed in a sealed chamber to prevent evaporation. After hybridization at 60°C for 6.5 hr, the slides were consecutively washed 3 times in a washing buffer of decreasing ionic strength.

The GEM system scanning. After hybridization, the GEM was scanned at 10-μm resolution to detect Cy3 and Cy5 fluorescence. Both Cy3 and Cy5 channels were scanned simultaneously with independent lasers. The emitted fluorescent light was optically filtered before photo-multiplier tubes translated the photons into an analog electrical signal, which was further processed into a 16-bit digital signal. This provided electronic images of both Cy3 and Cy5 with a 65,536-color resolution. A 16-color log scale was used for visual representation.

Normalization and ratio determination. Incyte GEM Tool software (Incyte) was

used for image analysis. A grid-and-region detection algorithm was used to determine the elements. The area surrounding each element image was used to calculate the local background and was subtracted from the total element signal. Background-subtracted element signals were used to calculate the Cy3:Cy5 ratio. The average of the resulting total Cy3 and Cy5 signals gives a ratio that is used to balance or normalize the signals.

Results of cDNA Microarray Analyses and Their Implications

In this study we investigated the changes in gene expression during and after benzene exposure (300 ppm). As previous studies (Yoon et al. 2001b) demonstrated that the *p53* tumor suppressor gene plays an important role in a cell response to benzene toxicity, analyses were performed using WT and p53-KO mice. In the sections that follow, we compare the gene expression profile obtained from WT mice using the Incyte GEM system with that obtained using the Affymetrix system, which in turn are compared with those of previous reports (Boley et al. 2002; Ho and Witz 1997; Schattenberg et al. 1994, Zhang et al. 2002). In addition we also describe particular genes related to p53-KO mice, such as cell cycle–regulating genes, apoptosis-related genes, and DNA repair–related genes.

All gene names, abbreviations, and accession numbers from MAS 4.0 are equivalent to those of GenBank (http://www.ncbi.nlm.nih/gov/Genbank/index.html).

Gene Expression Profile of Wild-Type Mice after Benzene Exposure

Figure 2 shows differences in the expression patterns of specific genes between, during, and after exposure of the WT mice to 300 ppm benzene for 2 weeks, determined using the Incyte GEM system (see Figure 1 for experimental schedule). Figure 2A shows the genes upregulated during benzene exposure (D5, D12), and then downregulated afterward (D+3), as represented by the *MPO* gene. Figure 2B shows the genes that had been continuously upregulated after benzene exposure, i.e., p53-binding protein 1 (*53BP1*), adenosine triphosphate (ATP)–binding cassette (ABC) transporter, and *N*-acetylglucosamine-6-*O*-sulfotransferase. Figure 2C shows the genes that had continuously been somewhat upregulated after benzene exposure, e.g., murine cathelin-like protein (*MCLP*), cell division cycle 2 (*cdc2*), and lipocalin 2. The expression patterns of *MPO* in Figure 2A may be induced by benzene metabolism during benzene exposure. This induction ceases after inhalation (Schattenberg et al. 1994), whereas *53BP1*, a DNA damage–responsive gene (Ward et al. 2003), and ABC transporter, a detoxifying drug–transporter (Ambudkar and Gottesman 1998), in Figure 2B show prolonged expressions after benzene exposure. *MCLP* (Gombert et al. 2003) and lipocalin 2 (Jessen and Stevens 2002) function as marker genes for differentiation. The genes listed in Figure 2C, including *cdc2*, may be upregulated for the proliferation of bone marrow cells during the recovery phase. A particular expression change in the aryl hydrocarbon receptor (AhR) was observed for which a mechanism could not be specified (data not shown). As we previously observed, sensitivity to benzene toxicity is innate in AhR-KO mice, implying that AhR transmits this sensitivity to benzene toxicity (Yoon et al. 2002).

The results of cDNA microarray analysis showed a broad consensus that the *p53* tumor suppressor gene is central to the mechanism of benzene action, by strictly regulating specific genes involved in the pathways of cell cycle arrest, apoptosis, and DNA repair. Such close association of the *p53* gene with the benzene toxicity mechanism raises the question: What would happen in mice whose *p53* gene is knocked out after benzene exposure? Thus, the cDNA microarray data obtained from the WT and p53-KO mice were applied to the Affymetrix system and analyzed using GeneSpring software, as described in "Materials and Methods." The results are shown in Table 1. This table shows that the expression profiles of the many genes involved in benzene metabolism, cell cycle or cell proliferation, and hemopoiesis in WT mice were generally consistent with the cDNA microarray data of C57BL/6 mice described in Table 2.

Characteristics of Gene Expression Profile of p53-KO Mice after Benzene Exposure

Mice lacking the *p53* gene and WT mice generally had similar expression patterns of the genes involved in benzene metabolism (CYP2E1 and MPO; Bernauer et al. 1999, 2000; Schattenberg et al. 1994; Yoon et al. 2001b) and hemopoiesis, suggesting that p53-KO mice are also affected to a similar extent by benzene exposure. This is consistent with the high frequency of micronuclei observed in benzene-exposed p53-deficient mice (Healy et al. 2001) (Table 1, Table 3A; p53-independent, benzene-induced gene expression level increase or decrease.). Figure 3 shows scatterplots representing the expression levels of genes in the bone marrow cells of the benzene-exposed WT (Figure 3A) and p53-KO mice (Figure 3B) relative to the expression levels of the genes in those of the corresponding sham-control mice. To elucidate and visualize the difference in gene expression level between the WT and p53-KO mice, clustering analysis was performed (Figure 4). The genes expressed include cell cycle/proliferation–associated genes. Table 3B lists the genes with a p53-dependent, benzene-induced decrease (e.g., G protein–coupled receptor [*GPCR*]) or increase (e.g., *caspase-11*) in expression level in the WT mice. In the

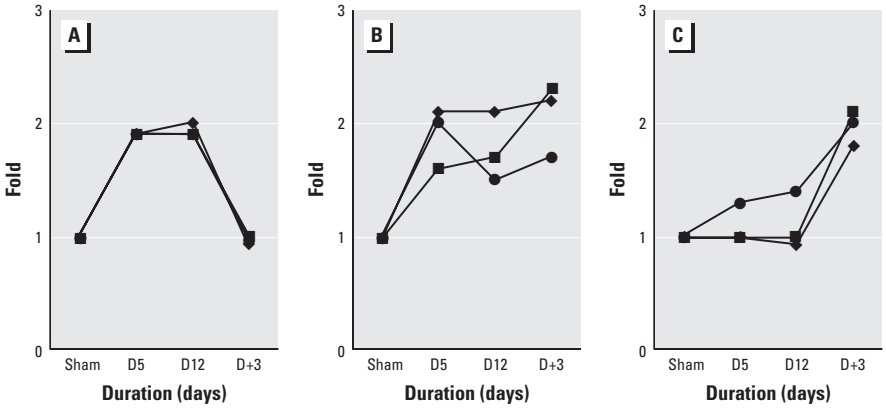

Figure 2. Three different expression patterns are shown along the time course. Benzene was used to expose the mice at 300 ppm for 1 week (D5) and 2 weeks (D12). D+3 designates the recovery group. The Incyte GEM system was used. Background-subtracted element signals were used to calculate the Cy3:Cy5 ratio. (*A*) Genes upregulated during the benzene exposure followed by immediate downregulation after benzene exposure: *MPO* (GenBank accession number X15313, [■]), *MPO* (GenBank accession number X15378, [◆]). (*B*) Genes upregulated during and after benzene exposure: *N*-acetylglucosamine-6-*O*-sulfotransferase (■), ABC transporter (◆), *53BP1* (●). (*C*) The genes were gradually or immediately upregulated after the benzene exposure, chiefly represented by DNA repair and proliferation during the recovery phase; *MCLP* (■), *cdc2* (◆), lipocalin 2 (●).

Table 1. Gene expression profiles in WT and p53-KO mice. Mice were exposed to 300 ppm benzene for 6 hr/day, 5 days/week, for 2 weeks, and killed on day 12.[a]

Category	Gene name[b]	Fold change WT	Fold change KO	Accession number
Cell cycle	*Calcyclin*	1.08	1.89	X66449
	Cyclin B1	0.85	1.48	X64713
	Cyclin D3	0.83	1.20	M86186
	Cyclin G1	1.67	1.32	L49507
	Dmp1	2.01	2.81	U70017
	Gadd 45[c]	1.63	(—)	U00937
	JNK2	1.07	1.82	AB005664
	KSR1; protein kinase related to Raf protein kinase	1.11	2.57	U43585
	mLimk1; *Mus musculus* protein kinase	2.67	1.18	X86569
	Mph1/Rae 28; polycomb binding protein	4.97	0.06	U63386
	Nsg1; similar to mouse *p21*	2.45	1.83	AV347030
	p21[c]	1.37	(—)	U09507
	p53	1.03	0.13	U59758
	PERK	0.81	1.63	AF076681
	SNK; serum inducible kinase	1.68	1.02	M96163
	Tsc-2	2.00	1.25	U37775
	Wee-1[c]	1.95	(—)	D30743
	Wig-1; *p53*-inducible zinc finger protein	1.83	0.07	AF012923
Growth factor	*EGFB-3*; epidermal growth factor binding protein 3	1.92	0.69	M17962
	GPCR; *EB11*	0.01	0.97	L31580
	Growth hormone	0.99	1.73	X02891
	IGFBP-6 (*s*)	2.88	0.10	X81584
	PGRP; tumor necrosis factor super family 3-like	0.95	1.80	AF076482
	Placental growth factor	1.13	2.14	X80171
DNA damage /repair	*Rad50*	1.23	0.40	U66887
	Rad51	0.72	0.08	AV311591
Apoptosis	*Apaf-1*	1.16	1.75	AF064071
	Bax-alpha	1.20	1.21	L22472
	Bcl-2 alpha	0.91	1.66	L31532
	Caspase-9	0.83	1.59	AB019600
	Caspase-9S	0.84	2.26	AB019601
	Caspase-11	2.49	1.22	Y13089
	Caspase-12	0.86	0.18	Y13090
	ELK1; member of ETS oncogene family	1.33	2.06	X87257
	Metaxin2	0.95	1.55	AF053550
	p58; protein kinase inhibitor (*PKI*)	1.55	0.81	U28423
	Smad6	1.36	1.92	AF010133
	Siva (proapoptotic protein)	0.88	1.62	AF033115
	WISP1	0.68	1.26	AF100777
	WISP2	0.83	8.32	AF100778
Oxidative stress	*Aldehyde dehydrogease 4*	1.07	2.44	U14390
	Cox5b	1.07	1.56	X53157
	Cox7a-L	0.97	1.51	AF037371
	Cui/Zn-SOD	1.19	1.63	M35725
	Glyceraldehyde-3-phosphate dehydrogenase	1.06	3.34	M32599
	LDH1; lactate dehydrogenase 1	1.13	2.34	AW123952
	LDH2; lactate dehydrogenase 2	0.97	1.72	X51905
	Metallothionein 1	4.89	0.93	V00835
Metabolic enzyme	*CYP2E1*	2.13	1.72	X01026
	CYP7B1	1.84	1.11	U36993
	MPO; myeloperoxidase	1.68	1.49	X15378
Hemopoiesis	*ALK-1*; TGF-beta type 1 receptor	2.53	2.71	Z31664
	Beta-spectrin 3	1.78	0.87	AF026489
	CD3-theta T cell receptor	1.07	2.37	L03353
	Fra-2; *fos*-related antigen 2	1.78	1.78	X83971
	IL-4	0.91	1.95	M25892
	M-CSF; macrophage colony-stimulating factor	1.03	2.13	M21952
	Mac-1 alpha	0.74	1.93	X07640
	Mg11; IFN-induced	0.88	1.75	U15635
	MTCP-1; mature T cell proliferation 1	1.52	1.28	Z35294
	NFAT-1; nuclear factor of activated T cells 1	0.60	2.02	U36576
	Phospholipase A_2	1.35	1.77	U18119
	PI3K catalytic subunit p110 delta	2.36	0.18	U86587
	S100 calcium-binding protein A13	1.24	1.78	X99921
	STAT5B	0.91	1.74	AJ237939
	TCF; T-cell factor, alternatively spliced	1.00	2.11	AF107298
	TNFRrp; lymphotoxin-beta receptor	2.06	1.71	L38423
	Nr1il; vitamin D receptor	2.54	1.60	D31969
Oncogene	*Fes*	0.81	1.79	X12616
	c-*fos*	1.57	0.94	V00727
	RAB17; member of *RAS* oncogene family	2.42	1.53	X70804
	Wnt-1/INT-1	1.72	1.23	M11943
Fatty acid β-oxidation	Acyl-CoA thioesterase	2.44	0.38	Y14004
	Adipose fatty acid binding protein	1.75	1.25	M20497

[a]The studies involved two to four animals; data were obtained from the use of the Affymetrix gene chips. Mice were killed on day 12, immediately after benzene exposure (see Figure 1, "Experimental Schedule"). [b]Information for GenBank (http://www.ncbi.nlm.nih.gov/Genbank/index.html). [c]No data available for p53-KO mice.

p53-KO mice, these genes did not change their expression level with benzene exposure. Table 3C shows that some changes in gene expression were undetectable because of the function of the *p53* gene, which can be "visualized" in the p53-KO microarray (Figure 4). Namely, data from toxicogenomics studies of specific gene KO mice could possibly disclose homeostatic balances undetectable in conventional WT mice.

Cell Cycle–Regulating Genes in p53-KO Mice and Wild-Type Mice

Cyclin genes were generally activated in p53-KO mice after benzene exposure, whereas cell cycle–regulating genes including the G2/M arrest-related gene *cyclin G1* (Kimura et al. 2001) were upregulated in WT mice. These findings indicate that the hemopoietic cell cycle is still functional in p53-KO mice during benzene exposure, whereas in WT mice it is arrested because of alterations in the expression of cell-cycle checkpoint genes, particularly the *p53* gene (Yoon et al. 2001b).

Some upstream genes encoding *p53*, such as *Dmp1* and *Raf-1* of the p53-KO mice, compared with those of the corresponding experimental groups of the WT mice, were upregulated to a similar extent or were more strongly enhanced in their expression. This is another indication of the role of the p53-mediated pathway in the mechanism of benzene toxicity associated with cell cycle regulation. Such information could be important in helping investigators to understand yet unknown mechanisms of chemical toxicity.

Table 2. Expression profiles of the genes.

Category	Gene name[a]	Reference
Metabolic enzyme	*CYP2E1*	Zhang et al. 2002
	MPO	Schattenberg et al. 1994
Cell cycle	*p53*	Boley et al. 2002
	p21 (*waf 1*)	Boley et al. 2002
	Cyclin G	Boley et al. 2002
	Gadd 45	Boley et al. 2002
Apoptosis	*Bax*-alpha	Boley et al. 2002
Oncogene	c-*fos*	Ho and Witz 1997

[a]Information for GenBank (http://www.ncbi.nlm.nih.gov/Genbank/index.html).

It is important to note that such a conclusion possibly can be drawn by carefully and simultaneously screening different expression patterns of many genes with interrelated functions, including genes showing small changes in expression levels (about 1.5- to 2-fold). The investigation of the expression levels of a limited number of genes generally may not provide insight into the main mechanism of chemical toxicity or clues to the particular role of each of the investigated genes in this mechanism. Toxicogenomics may have a strong advantage from this point of view (Inoue 2003).

Apoptosis-Related Genes in p53-KO Mice and Wild-Type Mice

The microarray analysis results of the p53-KO mice reminded us of the importance of the *p53* gene in the mechanism of benzene toxicity. The genes activated by the *p53* gene, including *p21*, *caspase 11* (Choi et al. 2001; Kang et al. 2000), and *cyclin G1* (Kimura et al. 2001), were distinctly upregulated in the benzene-exposed WT mice (Table 1). It is interesting that *caspase 11* instead of *caspase 9* was highly expressed after benzene exposure. This suggests that the p53-mediated activation of *caspase 11* is an important signaling pathway of apoptosis of bone marrow cells

Table 3. Differences in alteration of gene expression between WT and p53-KO mice after benzene exposure.

Expression category	Gene abbreviations[a]
A. p53-independent benzene-induced decrease or increase	
Decrease WT: decreased p53-KO: decreased	*CR6, EGFBP-1, GDIA, GDI-alpha, mGk-6, Glut-3, HDGF, PKD1, ZO-1*
Increase WT: increased p53-KO: increased	*ALK-1, Angrp, cardiac troponin T, Ctsg, CYP2E1, Dmp1, Fmo3, fra-2, GHR, Gpr50, Hox-1.7, KIK-I, MPO, NEFA protein, NrLi1, Nsg-1, PN-1, RAB17, Sim1, Sox10, Tip30, TNFRrp, WBP9*
B. p-53-dependent benzene-induced decrease or increase	
Decrease WT: decreased p53-KO: unchanged	*Adcy6, ApoE, AQ1*, B cell antigen receptor, *Cam III, CCR9, E2F1, FATP4, Fscn1, GPCR (EB11), Ig kappa light chain, IgA, IgH, mur42, Pdk1, PPT-B, Prkm1, TP, TRBF1*
Increase WT: increased p53-KO: unchanged	Adipose fatty acid binding protein, *Adh-3, caspase-11, cyclin G1, CYP7B1, EGFB-3, emp-1, FKBP23, c-fos, Hox-4.9, Int-1, Lfc, Krtl-12, mLimk1, MDC2, Mtcp1, Nr2b1, p58 (PKI), Pcnt, PFK, Pkacb, PGII, PTG, beta-spectrin, SPI-3, SNK, TSC-2*
C. p53-KO–related decrease or increase by benzene exposure but no changes in the WT mice	
Decrease WT: unchanged p53-KO: decreased	*CalDAG-GEFI, Cbfa2, Dctn1, Fr1, Grl-1, Ig/EBP, Klra3, Mek5,MEP,*
Increase WT: unchanged p53-KO: increased	*24p3, 4E-BP2, Abcg2, ACRP, activine, Ahd3, Alp, Anx3, AOE372, Apaf1, BAG-1, BAP, bcl-2, calcyclin, canexin, caspase 9, COX8H, caspase 9S, CCR1, CD3 theta, CD71, CD143, Cox5b, Cox7a1, Ctla-2a, Cu/Zn-SOD, cyclin B1, DCIR, Dnmt2, Dpagt2, E4BP4, EPO, FACS, Fes, elk1, G6PD, G6PD-2, Galbp, Gapdh, Gcdh, Gdi2,* growth hormone, *Gnb-1, Gng3lg, H-2T18, HES-1, IGF-1, IL1bc, IL-4, IL-9, JSR1, LDH-1, LDH-2, mLigl, Lipo 1, Lrf, Ly-3, Ly-40, Jam, JNK2, Kcc1, KSR1, M-CSF, Mac-1 alpha, Mch6, Mg11, MHR23A, MmCEN3, Mrad17, MRP14, Mtx2, NFATp, NL, Nmo1, OERK, PAFR, Pde8, PERK, PGRP, Pla2g2c, PLGF, Pop2, Prkm9, Prtn3, RBP-L, Rga, S100A13, Siva, Smad 6, SPRR2J, Stat4, Stat 5B, TCF4, TOM1, trypsin 2, Tst*

[a]Information for GenBank (http://www.ncbi.nlm.nih.gov/Genbank/index.html).

triggered by benzene exposure. This novel observation associated with the benzene toxicity mechanism together with the downmodulation of *caspase 12* was similarly addressed using WT and p53-KO mice in the study of the mechanism of chronic obstructive urinary disturbances (Choi et al. 2001). The decrease in the expression level of *caspase 12* in the p53-KO mice after benzene exposure seems to be in good agreement with the previous report on *caspase 12* regulation by p53 (Choi et al. 2001).

Genes associated with oxidative stress were both up- and downregulated in the p53-deficient mice, which may be an indication of benzene-induced oxidative stress (Yoon et al. 2001a; Table 1). It is not clear why oxidative stress–associated genes are activated in p53-KO mice and not in WT mice, but this might reflect the deregulation of the redox cycle due to the absence of the *p53* gene and the consecutive counteractivation of antioxidant enzymes (Chandel et al. 2000). Apoptotic protease-activating factor 1 (*Apaf-1*), metaxin, and *Siva* genes were also upregulated in the benzene-exposed p53-KO mice (Table 1). The expression of these genes may suggest proapoptotic conditions induced by benzene exposure of p53-KO mice. However, survival or anti-apoptosis genes such as *bcl-2*, *caspase 9S* (an endogenous dominant negative of *caspase 9*) (Seol and Billiar 1999), and *Smad6* (antagonist of tumor growth factor-β [TGF-β] signaling) (Imamura et al. 1997) are also activated in p53-KO mice. PERK (endoplasmic reticulum resident kinase) upregulation in p53-KO mice indicates the triggering of the unfolded protein-response signaling pathway, resulting in the loss of cyclin D1 (Brewer and Diehl 2000).

Expression of DNA Repair–Related Genes in *p53* Gene Network

Despite the possible damage to the DNA of the bone marrow cells of a p53-KO mouse, the DNA repair system is not likely to be functioning efficiently in the p53-KO mice, as DNA repair–related genes that were actively functioning in the benzene-exposed WT mice were not activated but rather suppressed in the p53-KO mice. In association with cell proliferation and apoptosis, high expression levels of the tuberous sclerosis gene (*Tsc-2*), a tumor suppressor gene encoding tuberin, and metallothionein 1 gene were noted in the WT mice (Table 1), raising the possibility that these genes are regulated by the *p53* gene. The association of metallothionein with p53 transcriptional activity has

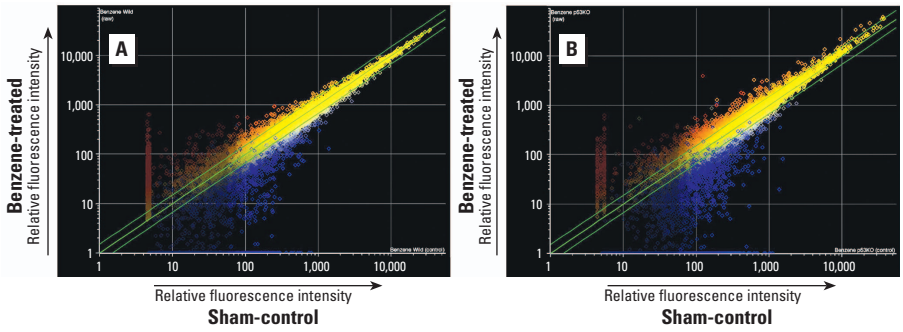

Figure 3. Scatterplots representing expression of genes in the bone marrow cells of benzene-exposed WT (*A*) and p53-KO mice (*B*) relative to expression of the genes in those of the corresponding sham-control mice, obtained using the Affymetrix system; *x*-axis and *y*-axis, respectively, indicate fluorescent signal intensity in the sham-control and benzene-exposed groups.

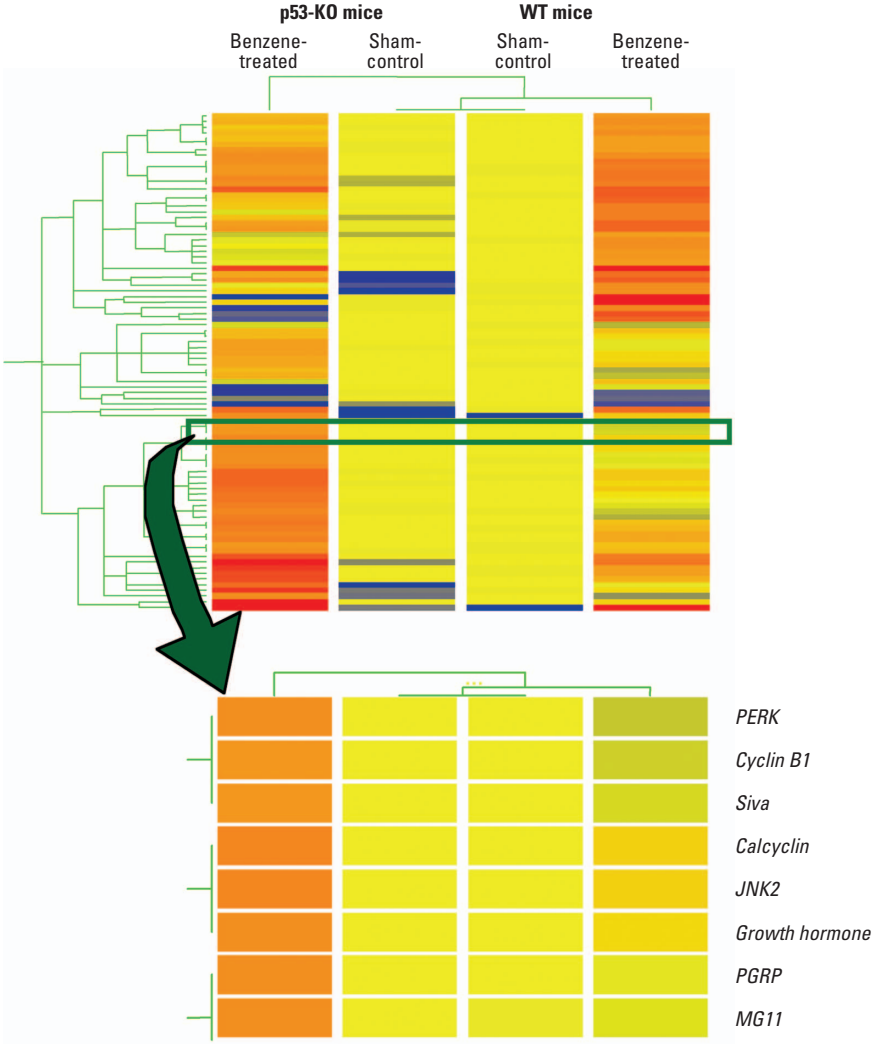

Figure 4. Clustering diagram of gene trees focused on particular genes of interest in the Affymetrix system. GeneSpring software was used to normalize the data. Clustering of microarray data revealed the standardized expression intensities of relevant genes shown by colors; from low expression level to high expression level, blue < yellow < orange < red. WT mice with or without benzene exposure, as well as p53-KO mice with or without benzene exposure are compared. A cluster of genes in the box (top) was found to consist of genes, the functions of which are related to cellular proliferation (bottom), and expressed only when p53 is knocked out, after benzene exposure. The average expression levels were obtained from two to four independent RNA samples from the mice. Genes in the box (top) are listed at the bottom; from the top: *PERK* (GenBank accession number AF076681), *cyclinB1* (GenBank accession number X64713), *Siva* (GenBank accession number AF033115), *calcyclin* (GenBank accession number X66449), *JNK2* (AB005664), growth hormone (GenBank accession number X02891), *PGRP* (GenBank accession number AF076482), *Mg11* (GenBank accession number U15635).

recently been postulated in an *in vitro* system in which metallothionein acts as a potent chelator to remove zinc from p53, thereby modulating p53 transcriptional activity (Meplan et al. 2000). The *Tsc-2* gene has recently been reported to regulate the insulin-signaling pathway mediated by protein kinase B (PKB/Akt) for cell growth (Gao and Pan 2001; Potter et al. 2002). It is noteworthy that *Tsc-2* is a target gene of 2,3,5-tris (glutathion-*S*-y) hydroquinone, a metabolite of hydroquinone for renal cell transformation (Lau et al. 2001). The high expression level of the *mph1/rae28* gene in the WT mice with severely suppressed bone marrow cellularity is noteworthy with respect to the maintenance of the activity of hemopoietic stem cells (Ohta et al. 2002). Furthermore, the Wnt-1 signaling pathway is also likely to be activated after benzene exposure, followed by the aberrant expressions of downstream genes such as *WISP1* and *WISP2* (Table 1). As the Wnt-1 signaling pathway was reported to regulate the proliferation and survival of various types of cell including B lymphocytes (Reya et al. 2000), the activation of both *mph1/rae28* and *Wnt-1* genes may be associated with the rapid recovery of suppressed bone marrow cellularity after cessation of benzene exposure.

Summary

As described above, the results of our cDNA microarray suggest that p53-KO mice are not resistant to benzene-induced toxic effects. These results were comparable with the dynamic protective responses of C57BL/6, WT mice at the gene functional level. On the basis of these observations, the effects of benzene on the bone marrow cells of p53-KO mice can be summarized as follows: *a*) cellular damage due to benzene metabolites and oxidative stress, *b*) dysfunction of the machinery of cell cycle arrest for repairing damaged DNA, resulting in continuous cycling of damaged cells even without undergoing repair, *c*) inhibition of apoptosis by both disruption of p53-dependent proapoptotic signaling and activation of survival genes, and *d*) failure of activating DNA repair genes. Such phenomena may lead to the increase in cell mutation frequencies at the candidate DNA locus, for instance, the *hprt* locus, responsible for benzene carcinogenesis, resulting in the development of hemopoietic malignancies. This hypothesis is based on multigene expression profiles that reasonably explain the high incidence and early onset of hemopoietic neoplasia, which were clearly observed in the p53 hetero- and homozygous KO mice chronically exposed to a critical dose of benzene for leukemogenicity tests (Kawasaki et al. Unpublished observation).

We also noted that the genes involved in fatty acid β oxidation such as the acyl-Co-A thioesterase gene and those encoding adipose fatty acid–binding proteins, which are commonly induced by peroxisome proliferators such as diethylhexylphthalate and clofibrate (Bartosiewicz et al. 2001), were also upregulated in the WT mice exposed to benzene (Table 1). A possible signaling pathway induced by benzene exposure is shown by a schematic in Figure 5. The present study using p53-KO mice elucidated the role of the *p53* gene not only in during benzene exposure, but also in the recovery state, and the gene expression profiling from p53-KO mice visualizes such oscillatory changes hidden behind the homeostatic balance organized by the *p53* gene in WT mice.

In conclusion, The cDNA microarray system used in this study revealed the mechanism of benzene toxicity by showing the altered expression of a number of benzene-affected genes including physiologic and toxicologic gene repertoires. Our data will provide valuable targets for the future investigation of the mechanism of benzene-induced toxicity and leukemogenicity.

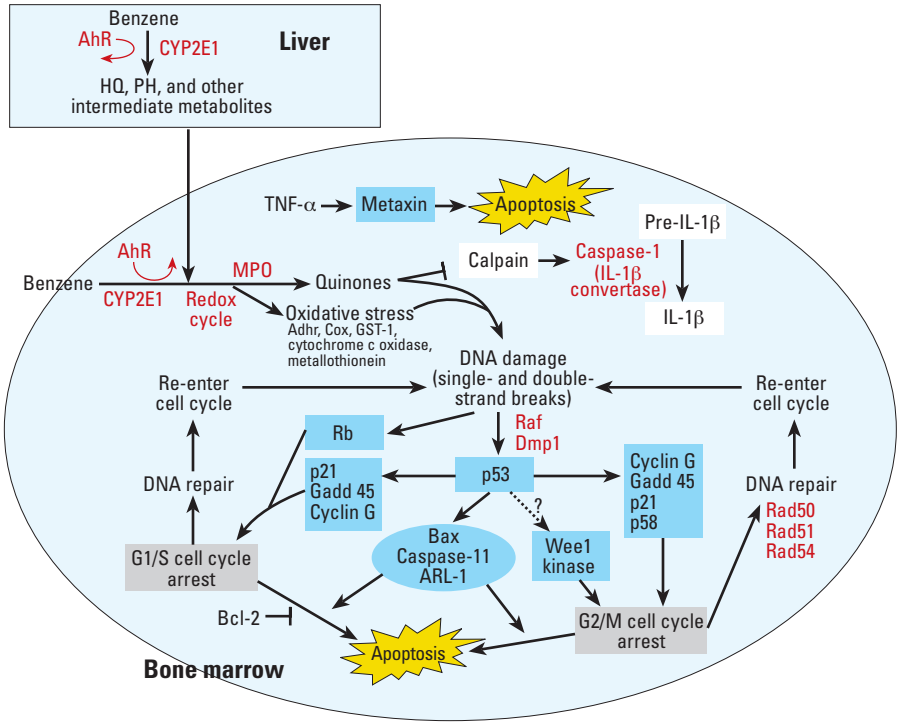

Figure 5. Mechanism of benzene toxicity at the molecular level based on the altered multigene expression profiles after benzene exposure. Benzene toxicity is dependent on AhR. CYP2E1 oxidizes benzene and produces quinones. Metabolites of benzene generated by cytochrome P450 monooxygenase and/or MPO trigger redox cycling consistent with the upregulation of genes for Adh4, Cox, glutathione *S*-transferase 1 (GST1) and metallothionein. Induction of p53 after DNA damage is the central toxicologic event, which readily induces the expression of p21, GADD45, and cyclin G, on one hand, the production of Bax, caspase 11, and ADP ribosylation factor–like protein 1 (ARL-1), and subsequently, the expression of Wee1 kinase. Induction of p21, in conjunction with Rb, results in the G1/S cell cycle arrest, whereas cyclin G and elongation factor 1 delta induces G2/M cell cycle arrest. Whether these cells in the cell cycle arrest further go into apoptosis or DNA repair depends on the participation of other cell signaling genes such as *bcl-2* and *Rad50*, *Rad51*, and *Rad54*. However, cells may mutate because of the possible failure of DNA repair.

References

Aksoy M, Erdem S, DinCol G. 1974. Leukemia in shoe-workers exposed chronically to benzene. Blood 44:837–841.

———. 1976. Types of leukemia in chronic benzene poisoning. A study in thirty-four patients. Acta Haematol 55:65–72.

Ambudkar SV, Gottesman MM, eds. ABC Transporters: Biochemical, Cellular, and Pharmacological Aspects. London:Academic Press, 1998.

Bartosiewicz MJ, Jenkins D, Penn S, Emery J, Buckpitt A. 2001. Unique gene expression patterns in liver and kidney associated with exposure to chemical toxicants. J Pharmacol Exp Ther 297:895–905.

Bernauer U, Vieth B, Ellrich R, Heinrich-Hirsch B, Janig GR, Gundert-Remy U. 1999. CYP2E1-dependent benzene toxicity: the role of extrahepatic benzene metabolism. Arch Toxicol 73:189–196.,

———. 2000. CYP2E1 expression in bone marrow and its intra- and interspecies variability: approaches for a more reliable extrapolation from one species to another in the risk assessment of chemicals. Arch Toxicol 73:618–624.

Boley SE, Wong VA, French JE, Recio L. 2002. p53 heterozygosity alters the mRNA expression of p53 target genes in the bone marrow in response to inhaled benzene. Toxicol Sci 66:209–215.

Brazma A, Hingamp P, Quackenbush J, Sherlock G, Spellman P, Stoeckert C, et al. 2001. Minimum information about a microarray experiment (MIAME)-toward standards for microarray data. Nat Genet 29:365–371.

Brewer JW, Diehl JA. 2000. PERK mediates cell-cycle exit during the mammalian unfolded protein response. Proc Natl Acad Sci USA 97:12625–12630.

Chandel NS, Vander Heiden MG, Thompson CB, Schumacker PT. 2000. Redox regulation of p53 during hypoxia. Oncogene 19:3840–3848.

Chen H, Eastmond DA. 1995. Synergistic increase in chromosomal breakage within the euchromatin induced by an interaction of the benzene metabolites phenol and hydroquinone in mice. Carcinogenesis 16:1963–1969.

Choi YJ, Mendoza L, Rha SJ, Sheikh-Hamad D, Baranowska-Daca E, Nguyen V, et al. 2001. Role of p53-dependent activation of caspases in chronic obstructive uropathy: evidence from p53 null mutant mice. J Am Soc Nephrol 12:983–992.

Cronkite EP, Bullis J, Inoue T, Drew RT. 1984. Benzene inhalation produces leukemia in mice. Toxicol Appl Pharmacol 75:358–361.

Cronkite EP, Drew RT, Inoue T, Hirabayashi Y, Bullis JE. 1989. Hematotoxicity and carcinogenicity of inhaled benzene. Environ Health Perspect 82:97–108.

Dean BJ. 1985. Recent findings on the genetic toxicology of benzene, toluene, xylenes and phenols. Mutat Res 154:153–181.

Eastmond DA, Smith MT, Irons RD. 1987. An interaction of benzene metabolites reproduces the myelotoxicity observed with benzene exposure. Toxicol Appl Pharmacol 91:85–95.

Farris GM, Robinson SN, Gaido KW, Wong BA, Wong VA, Hahn WP, et al. 1997. Benzene-induced hematotoxicity and bone marrow compensation in B6C3F1 mice. Fundam Appl Toxicol 36:119–129.

Gao X, Pan D. 2001. TSC1 and TSC2 tumor suppressors antagonize insulin signaling in cell growth. Genes Dev 15:1383–1392.

Gombart AF, Kwok SH, Anderson KL, Yamaguchi Y, Torbett BE, Koeffler HP. 2003. Regulation of neutrophil and eosinophil secondary granule gene expression by transcription factors C/EBP epsilon and PU.1. Blood 101:3265-3273.

Gut I, Nedelcheva V, Soucek P, Stopka P, Vodicka P, Gelboin HV, et al. 1996. The role of CYP2E1 and 2B1 in metabolic activation of benzene derivatives. Arch Toxicol 71:45–56.

Healy LN, Pluta LJ, James RA, Janszen DB, Torous D, French JE, et al. 2001. Induction and time-dependent accumulation of micronuclei in peripheral blood of transgenic p53+/– mice, Tg.AC (v-Ha-*ras*) and parental wild-type (C57BL/6 and FVB/N) mice exposed to benzene by inhalation. Mutagenesis 16:163–168.

Henderson RF. 1996. Species differences in the metabolism of benzene. Environ Health Perspect 104 (suppl 6):1173–1175.

Ho TY, Witz G. 1997. Increased gene expression in human promyeloid leukemia cells exposed to *trans,trans*-muconaldehyde, a hematotoxic benzene metabolite. Carcinogenesis 18:739–744.

Huff JE, Haseman JK, DeMarini DM, Eustis S, Maronpot RR, Peters AC, et al. 1989. Multiple-site carcinogenicity of benzene in Fischer 344 rats and B6C3F1 mice. Environ Health Perspect 82:125–163.

Imamura T, Takase M, Nishihara A, Oeda E, Hanai J, Kawabata M, et al. 1997. Smad6 inhibits signalling by the TGF-beta superfamily. Nature 389:622–626.

Inoue T. 2003. Introduction: Toxicogenomics—A New Paradigm of Toxicology. In: Toxicogenomics (Inoue T, Pennie WD, eds). Tokyo:Springer-Verlag, 3–11.

Jessen BA, Stevens GJ. 2002. Expression profiling during adipocyte differentiation of 3T3-L1 fibroblasts. Gene 299:95–100.

Kang SJ, Wang S, Hara H, Peterson EP, Namura S, Amin-Hanjani S, et al. 2000. Dual role of caspase-11 in mediating activation of caspase-1 and caspase-3 under pathological conditions. J Cell Biol 149: 613–622.

Kimura SH, Ikawa M, Ito A, Okabe M, Nojima H. 2001. Cyclin G1 is involved in G2/M arrest in response to DNA damage and in growth control after damage recovery. Oncogene 20:3290–3300

Kolachana P, Subrahmanyam VV, Meyer KB, Zhang L, Smith MT. 1993. Benzene and its phenolic metabolites produce oxidative DNA damage in HL60 cells *in vitro* and in the bone marrow *in vivo*. Cancer Res 53:1023–1026.

Laskin DL, Heck DE, Punjabi CJ, Laskin JD. 1996. Role of nitric oxide in hematosuppression and benzene-induced toxicity. Environ Health Perspect 104(suppl 6):1283–1287.

Lau SS, Monks TJ, Everitt JI, Kleymenova E, Walker CL. 2001. Carcinogenicity of a nephrotoxic metabolite of the "nongenotoxic" carcinogen hydroquinone. Chem Res Toxicol 14:25–33.

Lee EW, Garner CD. 1991. Effects of benzene on DNA strand breaks *in vivo* versus benzene metabolite-induced DNA strand breaks *in vitro* in mouse bone marrow cells. Toxicol Appl Pharmacol 108:497–508.

Low LK, Lambert C, Meeks J, Naro P, Mackerer CR. 1995. Tissue-specific metabolism of benzene in Zymbal gland and other solid tumor target tissues in rats. J Am Coll Toxicol 14:40–60.

Maltoni C, Ciliberti A, Cotti G, Conti B, Belpoggi F. 1989. Benzene, an experimental multipotential carcinogen: results of the long-term bioassays performed at the Bologna Institute of Oncology. Environ Health Perspect 82:109–124.

Meplan C, Richard MJ, Hainaut P. 2000. Metalloregulation of the tumor suppressor protein p53: zinc mediates the renaturation of p53 after exposure to metal chelators *in vitro* and in intact cells. Oncogene 19:5227–5236.

Moran JL, Siegel D, Sun XM, Ross D. 1996. Induction of apoptosis by benzene metabolites in HL60 and $CD34^+$ human bone marrow progenitor cells. Mol Pharmacol 50:610–615.

Niculescu R, Bradford HN, Colman RW, Kalf GF. 1995. Inhibition of the conversion of pre-interleukins-1 alpha and 1 beta to mature cytokines by *p*-benzoquinone, a metabolite of benzene. Chem Biol Interact 98:211–222.

Ohta H, Sawada A, Kim JY, Tokimasa S, Nishiguchi S, Humphries RK, et al. 2002. Polycomb group gene rae28 is required for sustaining activity of hematopoietic stem cells. J Exp Med 195:759–770.

Potter CJ, Pedraza LG, Xu T. 2002. Akt regulates growth by directly phosphorylating Tsc2. Nat Cell Biol 4:658–665.

Reya T, O'Riordan M, Okamura R, Devaney E, Willert K, Nusse R, et al. 2000. Wnt signaling regulates B lymphocyte proliferation through a LEF-1 dependent mechanism. Immunity 13:15–24.

Ross D. 2000. The role of metabolism and specific metabolites in benzene-induced toxicity: evidence and issues. J Toxicol Environ Health A 61:357–372.

Ross D, Siegel D, Schattenberg DG, Sun XM, Moran JL. 1996. Cell-specific activation and detoxification of benzene metabolites in mouse and human bone marrow: identification of target cells and a potential role for modulation of apoptosis in benzene toxicity. Environ Health Perspect 104(suppl 6):1177–1182.

Schattenberg DG, Stillman WS, Gruntmeir JJ, Helm KM, Irons RD, Ross D. 1994. Peroxidase activity in murine and human hematopoietic progenitor cells: potential relevance to benzene-induced toxicity. Mol Pharmacol 46:346–351.

Schlosser MJ, Shurina RD, Kalf GF. 1989. Metabolism of phenol and hydroquinone to reactive products by macrophage peroxidase or purified prostaglandin H synthase. Environ Health Perspect 82:229–237.

Schrenk D, Orzechowski A, Schwarz LR, Snyder R, Burchell B, Ingelman-Sundberg M, et al. 1996. Phase II metabolism of benzene. Environ Health Perspect 104(suppl 6):1183–1188.

Seol DW, Billiar TR. 1999. A caspase-9 variant missing the catalytic site is an endogenous inhibitor of apoptosis. J Biol Chem 274:2072–2076.

Smith MT, Yager JW, Steinmetz KL, Eastmond DA. 1989. Peroxidase-dependent metabolism of benzene's phenolic metabolites and its potential role in benzene toxicity and carcinogenicity. Environ Health Perspect 82:23–29.

Snyder CA, Goldstein BD, Sellakumar AR, Bromberg I, Laskin S, Albert RE. 1980. The inhalation toxicology of benzene: incidence of hematopoietic neoplasms and hematotoxicity in ARK/J and C57BL/6J mice. Toxicol Appl Pharmacol 54:323–331.

Snyder R, Hedli CC. 1996. An overview of benzene metabolism. Environ Health Perspect 104(suppl 6):1165–1171.

Snyder R, Kalf GF. 1994. A perspective on benzene leukemogenesis. Crit Rev Toxicol 24:177–209.

Subrahmanyam VV, Doane-Setzer P, Steinmetz KL, Ross D, Smith MT. 1990. Phenol-induced stimulation of hydroquinone bioactivation in mouse bone marrow *in vivo*: possible implications in benzene myelotoxicity. Toxicology 62:107–116.

Subrahmanyam VV, Ross D, Eastmond DA, Smith MT. 1991. Potential role of free radicals in benzene-induced myelotoxicity and leukemia. Free Radic Biol Med 11:495–515.

Tsukada T, Tomooka Y, Takai S, Ueda Y, Nishikawa S,

Yagi T, et al. 1993. Enhanced proliferative potential in culture of cells from p53-deficient mice. Oncogene 8:3313–3322.

Valentine JL, Lee SS, Seaton MJ, Asgharian B, Farris G, Corton JC, et al. 1996. Reduction of benzene metabolism and toxicity in mice that lack CYP2E1 expression. Toxicol Appl Pharmacol 141:205–213.

Vigliani EC, Forni A. 1976. Benzene and leukemia. Environ Res 11:122–127.

Ward IM, Minn K, van Deursen J, Chen J. 2003. p53 Binding protein 53BP1 is required for DNA damage responses and tumor suppression in mice. Mol Cell Biol 23:2556–2563.

Wolman SR. 1977. Cytologic and cytogenetic effects of benzene. J Toxicol Environ Health 2(suppl):63–68.

Yager JW, Eastmond DA, Robertson ML, Paradisin WM, Smith MT. 1990. Characterization of micronuclei induced in human lymphocytes by benzene metabolites. Cancer Res 50:393–399.

Yoon BI, Hirabayashi Y, Kaneko T, Kodama Y, Kanno J, Yodoi J, et al. 2001a. Transgene expression of thioredoxin (TRX/ADF) protects against 2,3,7,8-tetrachlorodibenzo-*p*-dioxin (TCDD)-induced hematotoxicity. Arch Environ Contam Toxicol 41:232–236.

Yoon BI, Hirabayashi Y, Kawasaki Y, Kodama Y, Kaneko T, Kanno J, et al. 2002. Aryl hydrocarbon receptor mediates benzene-induced hematotoxicity. Toxicol Sci 70:150–156.

Yoon BI, Hirabayashi Y, Kawasaki Y, Kodama Y, Kaneko T, Kim DY, et al. 2001b. Mechanism of action of benzene toxicity: cell cycle suppression in hemopoietic progenitor cells (CFU-GM). Exp Hematol 29:278–285.

Zhang S, Cawley GF, Eyer CS, Backes WL. 2002. Altered ethylbenzene-mediated hepatic CYP2E1 expression in growth hormone-deficient dwarf rats. Toxicol Appl Pharmacol 179:74–82.